Optical Particle Characterization in Flows

Cameron Tropea

Institute for Fluid Mechanics and Aerodynamics, Center of Smart Interfaces, Technische Universität Darmstadt, 64287 Darmstadt, Germany; email: ctropea@sla.tu-darmstadt.de

Annu. Rev. Fluid Mech. 2011. 43:399–426

First published online as a Review in Advance on September 14, 2010

The *Annual Review of Fluid Mechanics* is online at fluid.annualreviews.org

This article's doi:
10.1146/annurev-fluid-122109-160721

0066-4189/11/0115-0399$20.00

Keywords

light scattering, phase Doppler, LIF, particle sizing, interferometry, particle imaging, rainbow refractometry

Abstract

Particle characterization in dispersed multiphase flows is important in quantifying transport processes both in fundamental and applied research: Examples include atomization and spray processes, cavitation and bubbly flows, and solid particle transport in gas and liquid carrier phases. Optical techniques of particle characterization are preferred owing to their nonintrusiveness, and they can yield information about size, velocity, composition, and to some extent the shape of individual particles. This review focuses on recent advances for measuring size, temperature, and the composition of particles, including several planar methods, various imaging techniques, laser-induced fluorescence, and the more recent use of femtosecond pulsed light sources. It emphasizes the main sources of uncertainty, the achievable accuracy, and the outlook for improvement of specific techniques and for specific applications. Some remarks are also directed toward the computational tools used to design and investigate the performance of optical particle diagnostic instruments.

1. INTRODUCTION

Refractive index: an imaginary quantity, the imaginary part describing the absorption (attenuation) within the medium and the real part expressing the ratio of the speed of light in a vacuum to the speed in the medium

Geometric optics (GO): describes light propagation in terms of rays; is a good approximation when the wavelength is very small compared with the size of structures with which the light interacts

When speaking of optical particle characterization in flows, one usually interprets the term particle to mean a droplet, bubble, or a solid particle or indeed some combination of the three, such as a droplet with suspended solid particles. This already indicates the rather broad spectrum of flows and processes for which diagnostics for particle characterization can be in demand. The importance of particle characterization cannot be underestimated, not only in the process industry and quality control, but also in academic research. Fuel sprays, agricultural sprays, spray drying of foodstuffs or pharmaceuticals, domestic sprays, and spray cooling are just a few examples for which reliable knowledge about particle sizes or evaporation rates can be deciding factors in the performance or economy of a system. Whereas early optical diagnostics were restricted to the determination of velocity and number density of particles in a flow, estimates of size became feasible with a number of laser-based systems, and since then the characterization of particles has been extended for special situations to include temperature, concentration (for multicomponent/multiphase droplets), shape, and species. Nevertheless, today the determination of most of these quantities still remains a challenge; moreover, the associated measurement uncertainty is often quite difficult to quantify.

Optical diagnostics remains attractive because of the inherent nonintrusiveness, despite the necessity of optical access to the measurement location, and many experiments are designed specifically to accommodate this requirement. However, the field of optical particle characterization is broad and involves many applications not directly associated with fluid mechanics (e.g., analytic tasks, cytometry, reaction and cooling crystallization systems, and dynamic light scattering). The present review does not consider techniques for such applications, as well as those involving the bulk characterization of particle ensembles. The focus of this review remains on registering and characterizing single particles in a flow. Finally, the size range discussed encompasses those particles addressed when speaking of multiphase flows (i.e., approximately 0.5 μm to several hundred micrometers).

1.1. Statement of the Problem and Some Historical Remarks

We borrow Damaschke et al.'s (1998) pictorial classification of particles, in which the complexity of optical particle characterization becomes evident (**Figure 1**). Whereas for a homogeneous, spherical particle of known substance the diameter and the (complex) refractive index fully characterize the particle, for more complex particles additional parameters are required to describe shape, orientation, and composition. However, the mathematical description of a particle (shape, composition, optical properties) already poses challenges but is an essential first step to develop suitable diagnostic techniques, as indicated in **Figure 1**. The choice of model for different particle shapes will directly influence not only the chosen formulation of the light scattering, but also the information that is to be finally resolved in a measurement.

The second step involves a description of the light scattered from the particle. For homogeneous spherical particles, exact solutions of Maxwell's equations by Lorenz (1890) and Mie (1908) (van de Hulst 1981) yield a complete description of the scattered light from a plane incident wave. Debye (1908) interpreted the scattered light from a cylinder in terms of different scattering orders, and van der Pol & Bremmer (1937) generalized this for the sphere. For larger particles, light scattering can be approximated by geometric optics (GO) (Glantsching & Chen 1981, van de Hulst 1981). GO has been extended to describe smaller particles and to take into account diffraction and surface wave contributions to the scattering (Hovenac & Lock 1992, Borys et al. 1998). However, often laser beams are used as an illuminating source, and for many applications (i.e., when the beam waist is focused to the order of the particle diameter or smaller), the peculiarities of the laser beam (Kogelnik & Li 1966, Barton 1997) and their deviation from a plane wave must be taken into

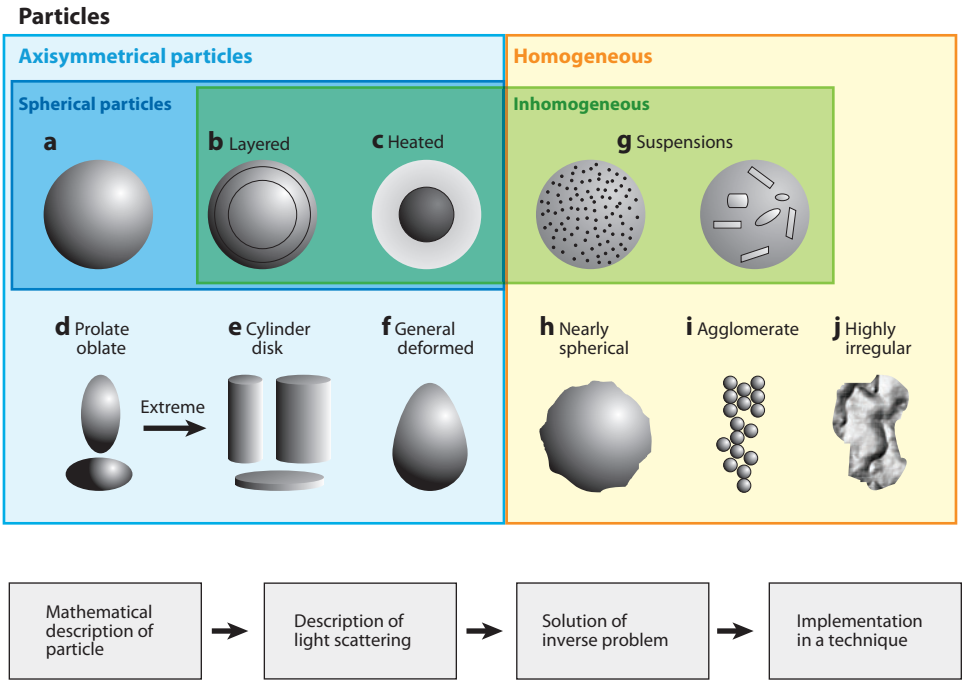

Figure 1

Classification of particles and steps toward diagnostic techniques.

account. Although this is conceptually straightforward using a GO approach, it is nevertheless tedious (Xu et al. 2006). Moreover, the wave (field) theory must be extended beyond the Lorenz-Mie theory when nonplanar waves are involved. Two approaches have been widely used, the Fourier-Lorenz-Mie theory (Albrecht et al. 1995, 2003) and the generalized Lorenz-Mie theory (Barton 1997, Gouesbet & Gréhan 1982, Gouesbet et al. 1988, Gouesbet 2009). Reviews of elastic light-scattering theories can be found in Wriedt (1998) and Gouesbet & Gréhan (2010) and their use in particle characterization in Jones (1999).

1.2. Some Basic Fundamentals of Light Scattering

Some basic principles of light scattering from particles may be helpful to understand the subsequent discussions. Optically the particle size range can be expressed in terms of the Mie scattering parameter x_m. The scattering ranges are Rayleigh ($x_m < 1$), GO ($x_m > 90$), and the intermediate range called the Mie region (**Figure 2**). The relative refractive index $m = n_p/n_o$ is the ratio of the refractive index of the particle to that of the surrounding medium and is a further parameter of influence for light scattering, being larger than unity for liquid droplets in gas and smaller than unity for gas bubbles in liquids.

The nonmonotonic dependence of scattered intensity on particle size (**Figure 2*a***) can be interpreted as the interference of various scattering orders (e.g., reflection and first-order refraction) in the far field, leading to interference fringes and resulting in intensity modulation. For GO, the various scattering orders can also be visualized as rays through the particle (**Figure 2*b***), leading to individual contributions to the total scattering intensity, depending on the scattering angle (**Figure 2*c***). The intensity of transmitted and reflected light at each interface is described by

Mie parameter: $x = d_p\pi/\lambda$, where d_p is the particle diameter and λ is the wavelength of light

Interference: the superposition of two or more waves resulting in a new wave pattern

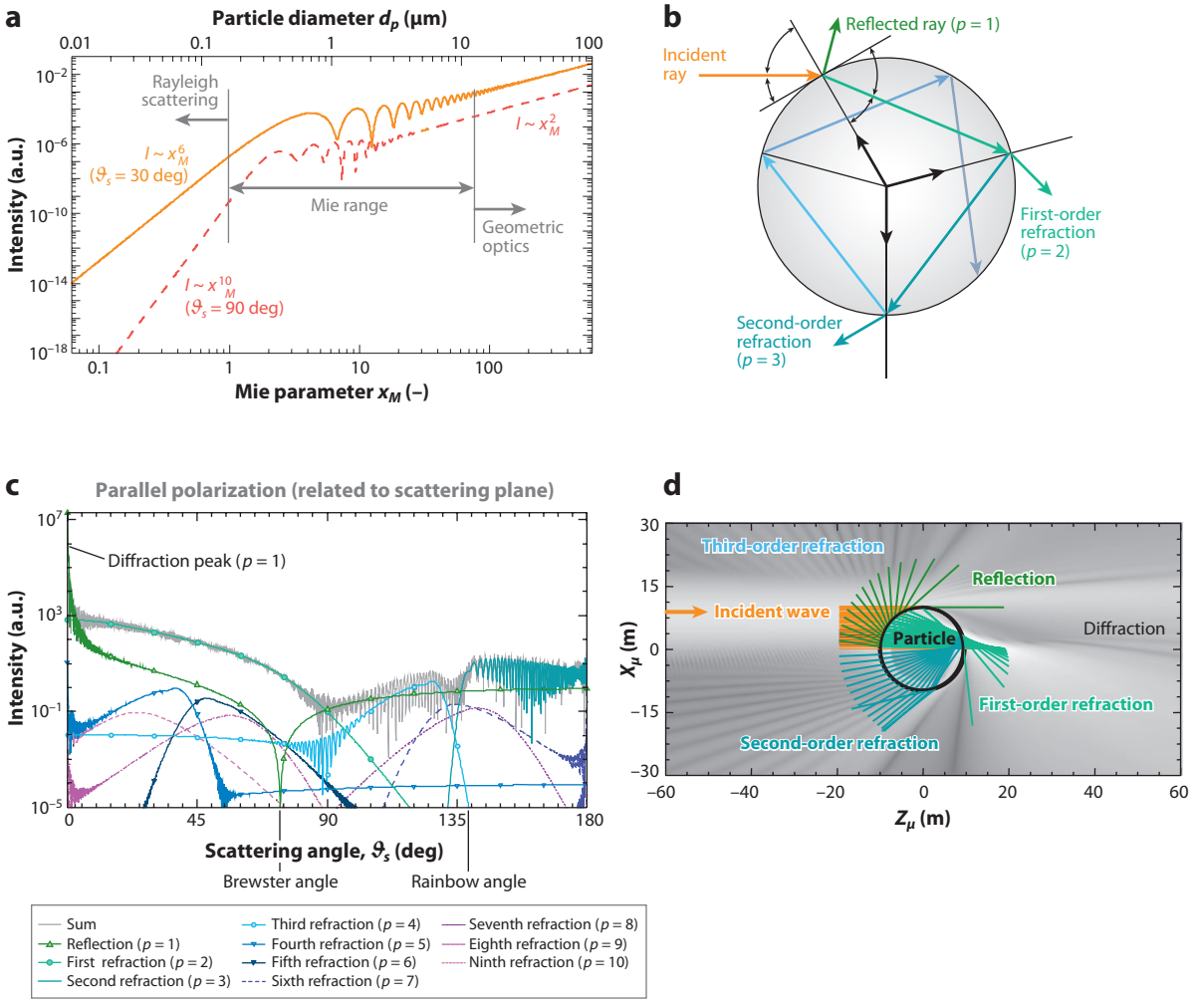

Figure 2

Illustration of scattering phenomena from a water droplet in air. (*a*) Scattered intensity as a function of the Mie parameter for two scattering angles υ_s ($m = 1.333 + j0.313$, parallel polarization, point detector). (*b*) Decomposition of an incident ray into reflection and refractive scattering orders according to geometric optics. (*c*) Scattered light intensity as a function of scattering angle, decomposed for the first 10 scattering orders calculated with Lorenz-Mie theory and Debye series decomposition for an incident plane wave ($d_p = 100$ μm, $\lambda = 488$ nm, $x = 643.8$, $m = 1.333$, point detector, parallel polarization). (*d*) Scattered intensity of the near field and internal field of a 20-μm droplet in a Gaussian beam of radius 5 μm ($d_p = 20$ μm, $m = 1.333$, $\lambda = 488$ nm, parallel polarization).

the Fresnel equations and is a function of relative refractive index and polarization (Hecht & Zajac 2003). The situation becomes more complex if a Gaussian beam of finite width (and not a plane wave) is incident (**Figure 2*d***), which is dealt with by using Fourier-Lorenz-Mie theory or generalized Lorenz-Mie theory.

Fresnel equations: describe the behavior of light when moving between media of differing refractive indices

1.3. Light Scattering by Nonspherical Particles

Calculation of light scattered by a nonspherical particle can be performed mainly by the use of variable-separation-based theories: surface-based or volume-based theories (Asano & Yamamoto

1975, Kerker 1988, Wriedt 1998). The variable-separation solution to light scattering is available for several regularly shaped particles following isolines of a certain type of orthogonal curvilinear coordinate system. For an arbitrary shaped particle, the boundary condition across the particle surface can still be imposed to apply the surface-based solutions [e.g., the T-matrix method (Doicu et al. 2000, Mischchenko et al. 2000), generalized multipole technique (Ludwig 1991), and moment method (Harrington 1968)]. For an irregularly shaped particle with complicated inhomogeneity, the particle and medium might be divided into grids for scattering calculation by use of volume-based solutions [e.g., finite-element method (Volakis et al. 1994), finite-difference time-domain method (Yee 1966), and discrete dipole approximation (Purcell & Pennypacker 1993)].

However, most electromagnetic theories for nonspherical particles lack computational efficiency for large particle sizes, in which case GO may be used complementarily. Moreover, they do not readily explain the physical mechanisms that cause various prominent intensity features. In contrast, the Debye series allows a detailed view of scattering by decomposing it into various orders, with each order p corresponding to the transmitted partial waves experiencing $(p - 1)$ internal reflections. In this way, one can identify the physical cause of various features of the Mie scattering curve, as well as their dependence on the particle properties. This physical insight gained from Debye theory is of great help in designing instruments in an optimal manner. As an extension of the Debye series for a sphere (van der Pol & Bremmer 1937), the Debye series for a nonspherical particle was recently developed by Xu et al. (2010).

2. MEASUREMENT TECHNIQUES

Table 1 presents an overview of optical particle characterization according to measurement principle and measured quantity. The most-suitable technique for a given application depends on many further factors, including required resolution and dynamic range, optical access, and particle concentration (Black et al. 1996, Damaschke et al. 2002b). Moreover, in most fluid mechanics applications, an estimate of flux density and/or concentration is required; hence a velocity measurement is generally also required, thus disqualifying some sizing techniques (e.g., diffraction-based instruments and laser-induced incandescence). Moreover, many techniques listed in **Table 1** are suitable only for particular conditions—in particular, the assumption of particle sphericity is frequent. Recent developments for a selection of these measurement principles are summarized in the following sections, beginning with the measurement of velocity, fluxes, and distributions and continuing with techniques for further scalar quantities. One overriding consideration in almost

Table 1 Overview of measurement techniques for optical particle characterization

Measurement principle	Measured quantity	Measurement technique
Direct imaging	Velocity, size, shape	PIV/PTV, shadowgraphy, glare-point separation
Intensity, intensity ratio	Size, temperature, species	Extinction/absorption, modulation depth, Mie/LIF ratio, two-band/three-band LIF
Interferometry	Velocity, size, refractive index/temperature	Laser Doppler, phase Doppler, ILIDS/IPI, diffraction, rainbow refractometry, holography
Time shift	Size, velocity	Time of flight, pulse displacement, time-shift technique
Pulse delay	Size, temperature	Femtosecond laser methods
Raman scattering	Temperature, species concentration	Raman spectroscopy

Abbreviations: ILIDS, interferometric laser imaging for droplet size; IPI, interferometric particle imaging; LIF, laser-induced fluorescence; PIV, particle image velocimetry; PTV, particle tracking velocimetry.

Fluorescence: the emission of electromagnetic radiation (light) by a substance that has absorbed radiation of a different wavelength

all the techniques discussed is the achievable measurement accuracy, and certainly with imaging techniques this depends heavily on the dynamic range, sensitivity, spatial resolution, and signal-to-noise ratio of the cameras and/or sensors employed (Hain et al. 2007). Indeed the technological developments in this area are certainly responsible in many ways for the current rapid progress in the field of optical particle characterization.

We note that the techniques listed in **Table 1** comprise both elastic scattering of light from particles and inelastic light scattering (e.g., fluorescence or Raman scattering). Inelastic scattering occurs when the scattered light is not of the same wavelength as the incident light; i.e., the incident photon interacts with the particle matter and transfers energy.

2.1. Measurement of Velocity, Fluxes, and Distributions

For the most part, velocity measurements are performed using either laser Doppler velocimetry (Albrecht et al. 2003) as a point measurement technique or particle image/particle tracking velocimetry (Raffel et al. 2007, Adrian & Westerweel 2010) as a whole-field technique. Time of flight through two or more volumes has also been used, whereby solutions exist in which more than one velocity component can be measured (Schodl & Förster 1988). Laser sheets rather than focused laser beams can be used for time-of-flight measurements to insure that oblique trajectories will also be properly registered. A velocity measurement is usually indispensible in particle characterization as flux density and concentration estimates require this information and, fluid dynamically speaking, the heat and mass transfer from the particle will depend on the relative velocity. This latter point suggests that the carrier velocity must be acquired independently, and this is often done by intentional and separate seeding of the carrier flow, with a laser Doppler or particle image/particle tracking velocimetry measurement distinguishing the second phase through wavelength or size if there is a significant size difference between phases. In particular, fluorescent particles can be used for one of the phases if wavelength differentiation is employed.

The measurement of distributions, flux density, and number concentration is essential to many applications, but it is also much more difficult than at first glance (Roisman & Tropea 2001). The flux density vector $\mathbf{q}$ of an arbitrary extensive scalar property P from N_p particles is

$$\mathbf{q}_P = \lim_{T\to\infty} \frac{1}{T} \sum_{i=1}^{N_{val}\le N_p} \frac{\eta_{val,i} P_i}{A_{val}(d_{p,i}, \mathbf{v}_{p,i})} \mathbf{e}_{v,i}, \tag{1}$$

where T is the total measurement time, N_{val} is the number of validated particles (not necessarily the number of particles, $N_p \ge N_{val}$), and $\mathbf{e}_{v,i}$ is the unit vector in the direction of particle motion. $\eta_{val,i}$ is the average number of particles corresponding to each validated signal i and is a correction factor accounting for the fact that if two or more particles are in the detection volume simultaneously, the signal processor may only register one particle (Roisman & Tropea 2001). Typical examples for the scalar property P are

$$P_i = 1 \qquad \text{(number)}, \tag{2a}$$

$$P_i = \frac{\pi \rho_p}{6} d_{p,i}^3 \qquad \text{(mass)}, \tag{2b}$$

$$P_i = \frac{\pi \rho_p}{12} d_{p,i}^3 \left|\mathbf{v}_{p,i}\right|^2 \qquad \text{(kinetic energy)}, \tag{2c}$$

where ρ is the density of the particle, and $\mathbf{v}_p$ is the vector velocity. We note that three velocity components are required in Equations 1 and 2 (for $\mathbf{e}_{v,i}$ and $\mathbf{v}_{p,i}$), unless a priori information is available about the velocity field. Furthermore, one can (and must) distinguish between a local distribution of particles at a particular instant in time (volume distribution) and a local distribution

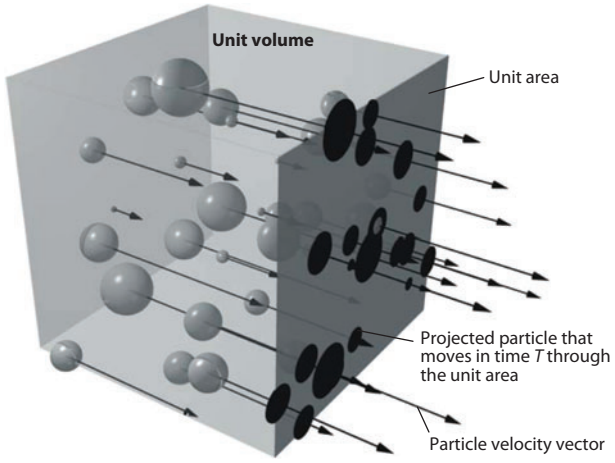

Figure 3

Visualization of local volume and flux density distributions. The particles that move through the unit area during time T are projected with dark circles. A positive correlation between particle size and particle velocity leads to a larger mean particle diameter in the flux density distribution than in the volume distribution. Small particles at the back of the unit volume do not cross the unit area in time T, whereas large particles do.

of particles crossing a unit area per unit time (flux density distribution), as illustrated in **Figure 3**. These two quantities are only the same if all the particles are convected with the same velocity.

Three main sources of error in the measurement of distributions, fluxes, and number concentration are errors in sizing, errors in counting (missed particles), and errors in knowing the reference area (or volume). Let us consider the estimation of reference area A_{val} (or volume). We speak of detection volume, as whether a particle is registered depends not only on the illuminated volume, but also on how the volume is imaged, the detector sensitivity, and the electronic signal (or image) processing software. For these reasons, a calibration is inevitably required to determine the detection area/volume. The real problem arises from the fact that the detection volume itself may be size dependent, as the scattered light intensity is size dependent, in the Mie range proportional to d^2 (large particles are seen, whereas small particles are not). Furthermore, most techniques involve the use of laser beams, which exhibit a Gaussian intensity profile (particles in the middle are seen, whereas particles at the edge are not).

This problem of estimator bias is equally severe for both point measurement techniques (e.g., phase Doppler) and whole-field imaging techniques with laser sheets. Unfortunately, validation through comparison with other techniques is difficult and requires extreme care in execution; even then error estimates from one study are seldom valid for the next (Dullenkopf et al. 1998, Widmann et al. 2001, Aísa et al. 2002). Overall, estimates of uncertainty of mass flux measurements range from 20% up to several hundred percent! This precludes the common expectation that, for instance, the evaporation rate in a spray can be measured by taking the difference in mass flux density on two downstream planes of a spray—the uncertainties are usually much larger than the expected measurement value.

2.2. Measurement of Scalar Quantities

The most frequent scalar quantity to be measured from each particle is its size; however, as **Table 1** indicates, temperature, species, refractive index, and shape are available with some

measurement techniques. In the following discussion these possibilities are discussed according to the respective measurement principle.

Glare points: the intensity maxima seen when a particle illuminated by a wide beam is viewed from a certain direction and imaged

Shaped beam: an illuminating beam for which the intensity or phase across the particle is not uniform

2.2.1. Direct imaging. Backlighting and image capture on a camera offer a viable means to estimate the size of a particle (shadowgraphy) (Bongiovanni et al. 1997, Hofeldt & Hanson 1991); several simultaneous views can be used for size estimation of nonspherical particles, and the appropriate depth of field can limit the detection volume. Velocity can be measured either by particle tracking between pulsed illuminations or by combining the shadowgraphy with a laser Doppler system, known as shadow Doppler velocimetry (Hardalupas et al. 1994, Jones et al. 2002, Matsuura et al. 2004), with both options commercially available. The latter solution has the advantage of being a pointwise measurement and presumably being applicable to higher particle concentrations, although systematic performance tests are not available (Morikita & Taylor 1998). Principally, shadowgraphy offers the advantage of measuring both nonspherical and nonhomogeneous particles, in that case employing more than one camera.

More recently, however, direct imaging of glare points has also become possible with the advent of fast, high-resolution cameras (van de Hulst & Wang 1991). This situation is illustrated schematically in **Figure 4**. Here the distance between glare points depends on the scattering angle at which the camera is placed and the relative refractive index, but then there exists a unique relation between glare-point distance and particle size. This technique, recognized very early (König et al. 1986, Hess 1998), has seen renewed interest because of its potential to be applicable in flows with higher particle concentration and to provide information about the shape of the particle. Recent work has employed polarization separation of glare points to extend the technique to smaller particles (Hess & L'Esperance 2009).

2.2.2. Intensity and intensity ratio. Intensity as a direct measure of particle size has always been plagued with difficulties, as detected intensity is dependent on so many other parameters of a flow system (e.g., trajectory of particle through a shaped beam/sheet, obscuration of incident and scattered light, extinction), despite some early attempts to remove the necessity of calibration (Farmer 1972, Bachalo 1980, Men et al. 1981, Hofeldt 1993). There is also the basic difficulty that, in the Mie scattering range, the intensity is not monotonically dependent on particle size (**Figure 2*a***).

Much more promising is the use of intensity ratio(s), in which common disturbing influences can be cancelled. The use of fluorescent tracers in droplets, and the assumption that the intensity of fluorescence is proportional to the droplet volume (d^3) while the ratio of Mie scattered light is proportional to d_p^2, a ratio of the intensities, distinguished by wavelength, will result in a size estimate (Yeh et al. 1993, Jermy & Greenhalgh 2000, Domann & Hardalupas 2001a,b). This technique, known as planar droplet sizing, has been pursued mostly using a laser light sheet and imaging cameras. More detailed studies confirm that for water or fuel droplets a scattering angle of $\upsilon_s = 90°$ is quite appropriate; however, the accuracy may depend on dye concentration and droplet size; therefore, a calibration becomes inevitable (Domann & Hardalupas 2001a). This suggests that the technique will encounter difficulties when droplets are evaporating and changing size, and this has been confirmed especially for smaller droplets ($d_p < 60$ μm). Estimates of achievable size accuracy for ideal conditions range from 10% to 30% (Domann & Hardalupas 2003).

Very recent work has explored the intensity of fluorescence when the illumination is a focused (shaped) beam rather than a uniform sheet, and for such an arrangement the particle size information is contained not only in the signal amplitude but also in its duration, assuming a velocity measurement can also be made (Frackowiak & Tropea 2010a,b). This then removes the pure (problematic) intensity dependence. What has become clear in these and earlier studies is that

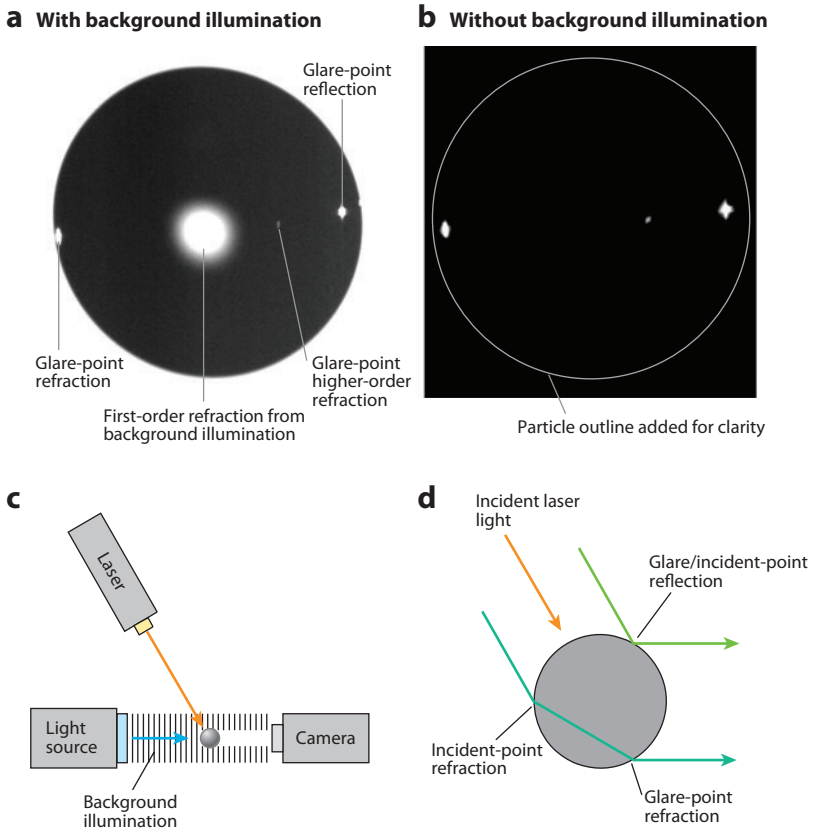

Figure 4

Schematic visualization of glare points for a water droplet in air, detected at an off-axis angle of $\vartheta_s = 30°$: (*a*) with background illumination and (*b*) without background illumination. The shape of the particle is indicated. (*c*) Schematic configuration of camera and light sources. (*d*) Light paths and generation of incident and glare points of reflection and refraction.

the fluorescent signal is not proportional to d_p^3: due to absorption, focusing of the incident light (especially for small particles), and the imaging detectors not seeing the entire inner volume of the particle for any given scattering angle. These blind spots in the particle arise because of the lens effect given by the particle interface, which is understandably more prominent with smaller particles.

Laser-induced fluorescence (LIF) as an intensity method is also widely used for temperature measurements of droplets (Murray & Melton 1985), temperature gradient measurements (Castanet et al. 2003, 2005), and, to some extent, species and concentration of multicomponent droplets (Maqua et al. 2007). In particular, when fluorescent dyes are used to detect both vaporized and liquid phases, a careful choice of dyes must be made (Coppeta & Rogers 1998, Düwel et al. 2003, Schulz & Sick 2005, Deprédurand et al. 2008). Whereas initial attempts for size and concentration measurements were also based on intensity (Bazile & Stepowski 1994, 1995; Lemoine et al. 1999), much more accurate measurements were obtained by introducing two-color (Hishida & Sakakibara 2000, Lavieille et al. 2001) and three-color (Maqua et al. 2007, Labergue et al. 2008) LIF from single dyes or ratiometric schemes from two different dyes (Coppeta & Rogers 1998).

LIF: laser-induced fluorescence

Brewster angle: the angle of incidence at which light with a particular polarization is perfectly transmitted through a surface, with no reflection [equal to $\pi - 2\arctan(m)$]

The basic principle behind such techniques rests on the temperature dependence of the fluorescence quantum yield. By taking the ratio of detector signals at two or three different bandwidths, one can cancel out other influencing factors. Using three colors, Lavieille et al. (2004) removed the influences of local laser power, tracer concentration, probe volume size, and Beer-Lambert absorption of the incident intensity, although some dependencies remained on size, which is of importance for evaporating sprays (Labergue et al. 2010). This ratiometric technique, combined with laser Doppler velocimetry, is commercially available.

2.2.3. Interferometry. A rather large number of measurement techniques fall under the general classification of interferometry (see **Table 1**), of which the phase Doppler technique, since its inception in 1981 (Flögel 1981, Bauckhage & Flögel 1984, Saffmann et al. 1984, Bachalo & Houser 1984), has become a de facto standard in sizing homogeneous, spherical particles. The phase Doppler technique is based on the interference of the same scattering order from two beams incident on the particle; a velocity measurement follows from the laser Doppler arrangement inherent in the system. The phase Doppler technique is normally considered a pointwise measurement, although the same principle can be implemented using two intersecting laser sheets, known as the global phase Doppler technique (Damaschke et al. 2005).

The measurement principle of phase Doppler can be exploited using various optical configurations, as indicated in **Figure 5**. The detector position is chosen at an off-axis scattering angle (φ) for which one scattering order dominates. For the example of water in air, **Figure 2*c*** indicates that, with parallel polarized light, an angle of 73° (Brewster angle) would be appropriate, as first-order refractive light ($p = 2$) dominates completely. Each laser beam exhibits a glare point for this order on a meridial line of the sphere and in the far field (out of focus). This leads to interference fringes, whose separation is inversely proportional to the particle diameter. For the standard phase Doppler arrangement (**Figure 5*a***), the phase difference between fringes on two detectors placed at the elevation angles $\pm\psi$ is then equal to

$$\Delta\Phi^{(p=2)} \approx -2\frac{2\pi}{\lambda} d_p \frac{m \sin\psi \sin{}^{\theta}\!/_{2}}{\nu\sqrt{1+m^2-m\nu}}, \quad \nu = \sqrt{2}\sqrt{1+\cos\psi\cos\phi\cos{}^{\theta}\!/_{2}}. \tag{3}$$

The proportionality constant between the measured phase difference and diameter contains only geometric quantities; hence the phase Doppler technique is often considered calibration free, although the overall accuracy is often determined by the accuracy of the angles in Equation 3. The intersecting laser beams also form a laser Doppler measurement volume; hence the frequency of the resulting signal corresponds linearly to the particle velocity. Two typical high-pass filtered Doppler signals exhibiting such a phase shift are illustrated in **Figure 5*d***. In the standard arrangement, a third detector is added to resolve the 2π ambiguity in the phase difference measurement.

Alternatively, the detectors can be arranged in the plane of the intersecting incident beams, in which case the detectors have the same elevation angle but two different scattering angles, which also results in a phase difference between the received signals. The glare points for these signals lie on an equatorial plane of the particle. The combination of the two optical configurations is known as the dual-mode phase Doppler (Tropea et al. 1996). Comparing the phase shift measured using the pair of detectors with the standard phase Doppler with the phase shift from the planar phase Doppler allows one to detect the sphericity of the particle (**Figure 5*c***). Indeed, this sensitivity to sphericity is one of the primary advantages of the dual-mode arrangement (Damaschke et al. 1998). Of course, a second velocity component is automatically available, which is essential for increasing the accuracy of flux density measurements, as mentioned in Section 2.1. The accuracy of the size measurement under ideal conditions can be reduced to less than 1%. Estimates of tolerable particle concentrations using the phase Doppler technique range from 10 particles mm^{-3} to

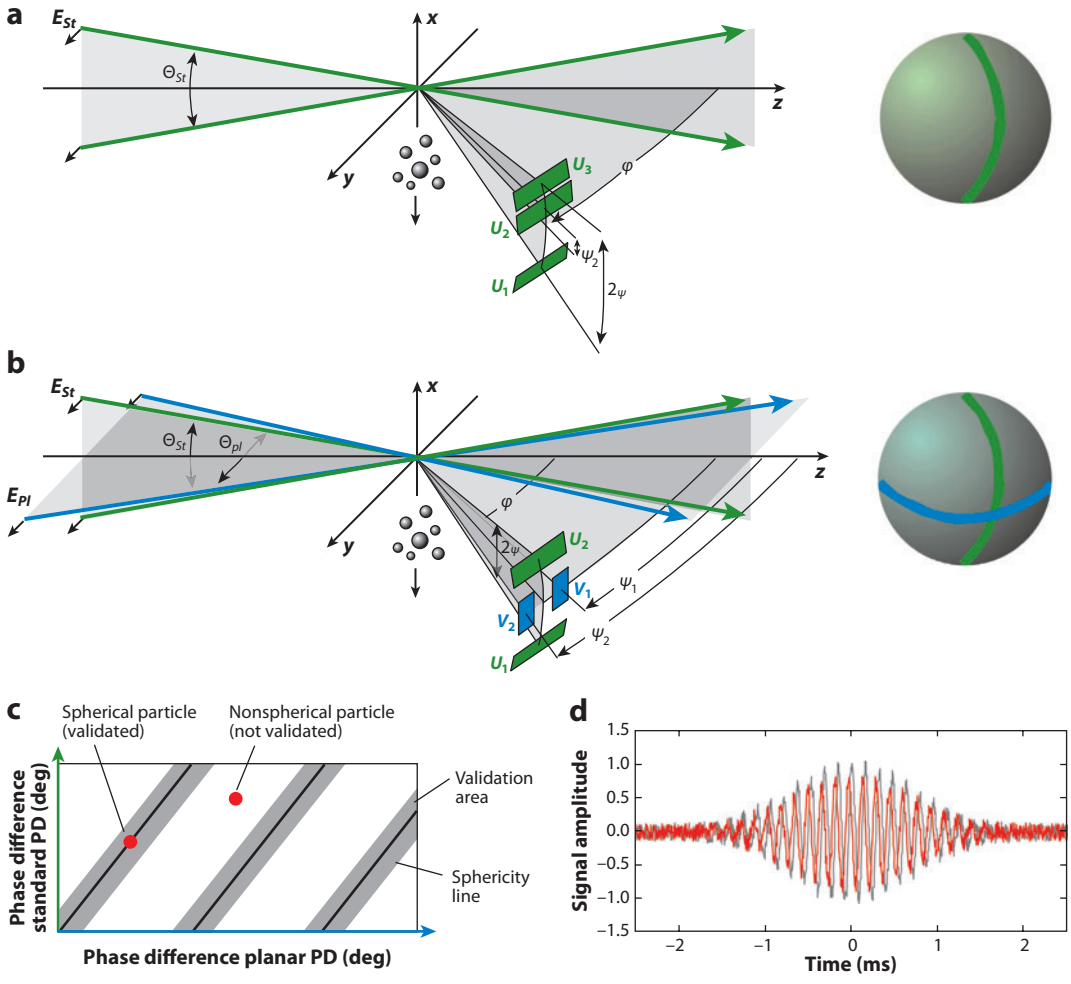

Figure 5

Optical configuration of the (*a*) standard (three detector) phase Doppler and the (*b*) dual-mode (standard plus planar) phase Doppler. (*c*) The sphericity validation of the measurement. (*d*) Phase-shifted signals from two detectors.

100 particles mm^{-3}. The actual limit depends in a complex manner on many factors, including the size distribution itself. Improvements to the realizable concentration limits have been achieved by restricting the detection volume on the receiver side using slit apertures.

It is important to note that if any refractive scattering orders are used in setting up the phase Doppler system (i.e., if reflection is not used), then the phase difference will depend on the relative refractive index (see Equation 3). In principle, therefore, by building in redundancy of the phase measurement, an estimate of the relative refractive index can be made. This may be interesting for distinguishing between dissimilar particles in a flow, but the estimates are generally not accurate enough to deduce the temperature of the particle (e.g., for a liquid droplet) from the relative refractive index. There have been many suggestions for building in redundancy while still maintaining a spherical validation. These include adding further detectors at additional scattering angles, known as the extended phase Doppler (Durst & Naqwi 1990, Pitcher et al. 1990,

ILIDS: interferometric laser imaging for droplet sizing

IPI: interferometric particle imaging

Naqwi et al. 1991, Volkholz et al. 1998). Onofri et al. (1996) suggested a combination of the phase Doppler technique with the time-shift technique in which scattering angles for the detectors are chosen such that signals from two different scattering orders—typically reflection and first-order refraction—are received separated in time. The time shift, as discussed in more detail below, arises by insuring that the incident beam is focused so that it is the same order in size as the particle, or smaller. Thus the redundancy of measurement is obtained by using two different scattering orders separated in time as the particle passes through the measurement volume, which has been termed the dual-burst technique (Onofri et al. 1998). In principle, also the absorption coefficient of light in the particle can be estimated from the difference in amplitude between the reflected signals and refracted signals, albeit with the usual difficulties involved in amplitude methods, as indicated above.

The time-shift effect exploited by Onofri et al. (1996) for extending the capabilities of the phase Doppler technique arises in a less desirable situation whenever the particle size becomes larger than the measurement volume dimensions. If the contributions to the signals arising from different scattering orders are not clearly separated in time but overlap, then the phase difference is some mixture between that expected for the various scattering orders, again typically involving reflected and first-order refracted light. This leads to erroneous estimates of the particle diameter and was first recognized by Saffmann (1986) and termed the trajectory effect. Other authors studied this effect in detail, sometimes calling it the Gaussian beam defect/effect (Sankar & Bachalo 1991, Gréhan et al. 1993, Albrecht et al. 1996).

There have been a number of strategies to alleviate this source of error. One suggestion is to monitor the amplitude of the signal (Sankar et al. 1992). A large particle erroneously detected using a wrong scattering mode due to its trajectory will yield a low signal amplitude. A size-dependent amplitude threshold could eliminate such errors. Several other suggestions are based essentially on building up redundancy in the measurement (Aizu et al. 1993, Xu & Tropea 1994), and one suggestion avoids the effect by adding detectors at a certain position, such that the ratio of the respective phase differences is no longer affected by trajectory (Qiu & Hsu 1999). Of course, the most reliable approach to avoid such errors is to insure that the measurement volume is always considerably larger than the largest particle to be sized.

Another technique similar to the phase Doppler technique, but involving the interference of two scattering orders from a single illuminating beam, is also becoming more widely used, usually implemented in a planar configuration. This technique has its origins in König et al. (1986), Ragucci et al. (1990), and Anders et al. (1991) and later in Glover et al. (1995), who termed the technique ILIDS (interferometric laser imaging for droplet sizing), despite the fact that the technique is not limited to the sizing of droplets. A more general designation is interferometric particle imaging (IPI). The measurement principle can be immediately understood by examining **Figure 4** and imagining the two glare points on the surface of the particle as two light sources. In the far field, these two glare points result in interference fringes, whose spacing will depend on the glare-point distance and some additional, known optical parameters, including the relative refractive index of the particle. This principle is illustrated schematically in **Figure 6*a***, in which the far-field interference is seen by defocusing the glare-point images from **Figure 4**. An image obtained from a laser sheet intersecting a water spray is shown in **Figure 6*c***, whereby the fringe spacing in each droplet image is inversely proportional to the particle size (Semidetnov & Tropea 2004). The out-of-focus image size of each particle is related to the position of the particle on the optical axis, which is, however, not easy to measure with a high degree of accuracy. Combining the planar laser illumination for the IPI with a pulsed operation allows the particle velocity to be determined (particle tracking), and by monitoring the change of particle image size, one can also estimate the third velocity component.

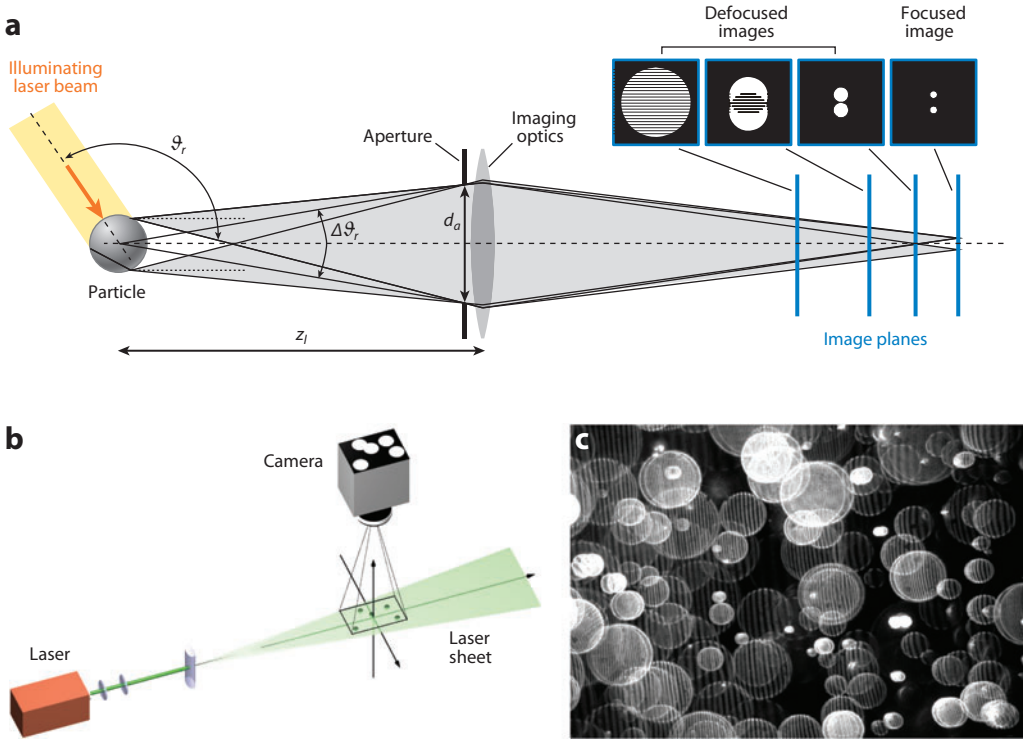

Figure 6

Interferometric particle imaging (IPI). (*a*) Measurement principle, using an out-of-focus image of glare points from two scattering orders. (*b*) Optical arrangement. (*c*) Planar IPI image from a water spray. The fringe spacing is inversely proportional to the particle size.

More recent work has introduced so-called optical compression to increase the measurable particle concentration limits of the technique, as well as made further improvements in the signal processing (Maeda et al. 2000, 2002; Kawaguchi et al. 2002). Nevertheless, this technique and the global phase Doppler technique exhibit significantly lower measurable concentration limits than the phase Doppler technique (Damaschke et al. 2002b).

The IPI technique is expected to have a similar sensitivity to the nonsphericity of particles as the phase Doppler technique, although a rigorous study has not been performed to date. One distinct advantage of IPI over the phase Doppler technique is that the coherence length of the illuminating beam/sheet need not be much longer than the dimension of the particle, because this is the maximum path-length difference involved in producing the interference fringes. Nevertheless, a collection angle must still be chosen such that the two scattering orders involved are approximately equal in intensity; otherwise the modulation depth of the interference fringes suffers, leading ultimately to a lower signal-to-noise ratio (i.e., higher measurement uncertainty of size). Fortunately, for liquids with a relative refractive index that is approximately that of water in air ($m = 1.33$), a 90° collection angle is quite appropriate, which is seen in **Figure 2*c*** by comparing the amplitude of the reflected and first-order refracted light at a 90° scattering angle.

If the global phase Doppler or IPI technique is used in combination with particle tracking, then the position of the out-of-focus particle images must be determined with high accuracy, which turns out to be quite difficult, especially at higher concentrations at which considerable image overlap occurs. In this case it is advantageous to use two cameras, one in focus and another out

of focus, to determine the particle position in the camera plane to a higher degree of accuracy. This combination of IPI and particle image/particle tracking velocimetry can also be extended to include tracer particles in the carrier phase, hence allowing the velocity of two phases (i.e., relative velocity) to be measured with one optical system (Hardalupas et al. 2010).

CCD: charge-coupled device

Rainbow: the interference of two rays of the same scattering order passing through the particle on different paths but exiting with the same scattering angle

Particle sizing using holography is not new (Thomson 1974, Jones et al. 1978, Shimizu et al. 1982), but the technique became significantly more attractive with the advent of digital holography (Schnars & Jüptner 2002, Kühn et al. 2008) and digital in-line holography (Müller et al. 2004, Garcia-Sucerquia et al. 2006, Sheng et al. 2006), the latter simplifying the optical arrangement greatly. For in-line holography, an expanded laser beam is passed through the measurement volume (e.g., a spray). The undistorted part of the beam arriving at the CCD (charge-coupled device) camera is the reference beam, and the part diffracted by the particles is the object beam. The interference is described by the Fresnel-Kirchoff integral (Schnars & Jüptner 2005). Noise from secondary scattering can be reduced using various optical filters and enhancement routines (Denis et al. 2005, Singh & Asundi 2005, Kim & Lee 2006). The focal plane of any individual particle, i.e., the position of the particle along the optical axis, can be found using various techniques based on either amplitude (Lefebvre et al. 2000, Dubois et al. 2006) or on cross-correlations of images taken at sequential slices along the optical axis (Choo & Kang 2006).

The current state of the art is well summarized by Palero et al. (2005, 2007), Garcia-Sucerquia et al. (2006), and Sheng & Katz (2010). Palero et al. (2007) concluded that digital in-line holography is well suited for particle characterization in systems with low particle concentration. The accuracy in the measured droplet size is approximately 5% for digital in-line holography and 1.6% for digital image plane holography, whereby estimated allowable particle concentrations are approximately 70 particles mm^{-3} for a 1-mm-thick plane illumination. Examples of sizing and tracking other, at times unconventional, particles using digital holographic methods are also abundant (Heydt et al. 2007, Sheng et al. 2007).

The rainbow phenomenon has also been employed for both particle sizing and estimation of refractive index (or temperature). One common use is the rainbow arising from second-order refraction, as illustrated in **Figure 7** and also in **Figure 2*c*** for the case of a water droplet in air ($\vartheta_s = 137°$). Ideally the position of the rainbow is dependent only on the relative refractive index and can be measured with an appropriate line detector or camera. The particle diameter influences the angular frequency of the intensity maxima, as expected from **Figure 7**.

In terms of exploiting the rainbow for diagnostics, the situation is complicated by several factors. To begin with, the inflection point of the curve, not the angular rainbow position, is independent of particle diameter (see **Figure 7*b***) (Roth et al. 1996). However, a more severe concern is the appearance of additional interference phenomena arising from further scattering modes. In particular, the reflection interferes with the second-order refraction to create a ripple structure on the rainbow, which was pointed out in detail by van Beeck & Riethmuller (1996). As the particle becomes smaller, the frequency of the ripple structure approaches that of the supernumerary bows of the main rainbow, and the uncertainty in determining the position of the rainbow becomes intolerably large. Several remedies have been proposed, including to use a low-pass filter (Roth et al. 1991), to curve-fit the primary fringe of the rainbow (Sankar et al. 1993), and, more recently, to fit the measured signal to Nussenzveig's (1969a,b) theory, taking into account the ripple structure (Saengkaew et al. 2010). Section 2.2.5 outlines another solution using femtosecond or short–coherence length light sources. Attempts to improve the measurement accuracy of the refractive index have included the combination of rainbow refractometry with a phase Doppler system for particle velocity and size measurement, which has also been commercially offered (Sankar et al. 1993, van Beeck & Riethmuller 1996).

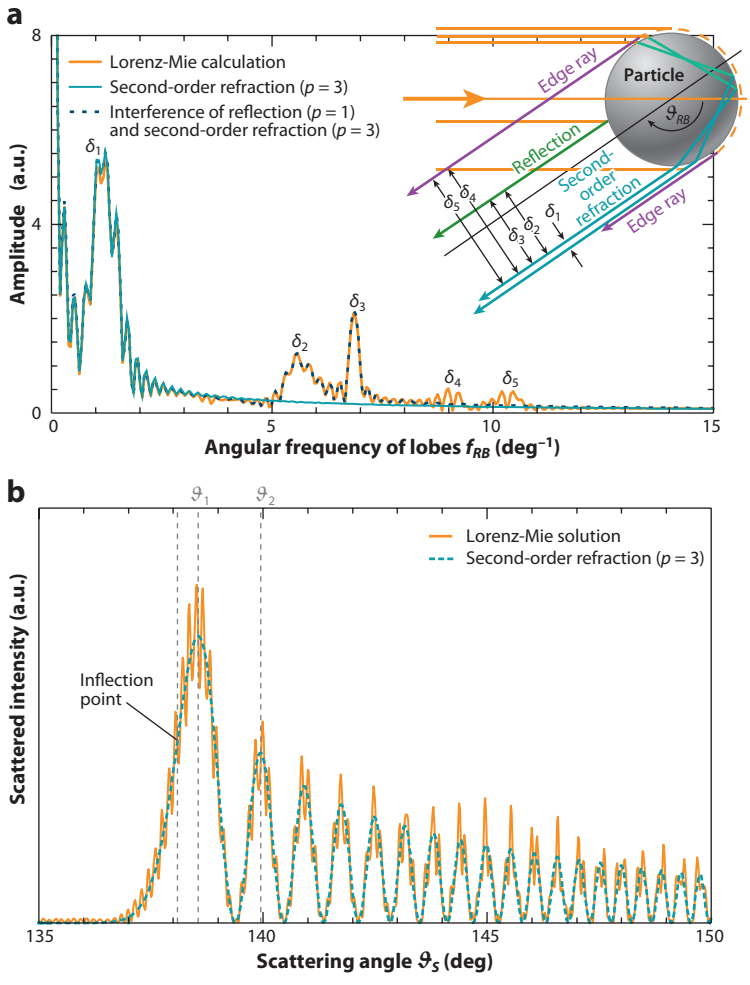

Figure 7

(*a*) Rays contributing to the primary rainbow and the rainbow spectrum generated by the interference of rays from reflection, second-order refraction, and surface waves. (*b*) The rainbow computed using Lorenz-Mie theory and second-order refraction from Debye series decomposition (300 μm, $\lambda = 488$ nm, and $m = 1.333$, with perpendicular polarization).

Nevertheless, the most severe drawback of rainbow refractometry is its extreme sensitivity to the nonsphericity of the particle, as recognized by Marsten (1980). Van Beeck et al. (1999, 2001) introduced global rainbow refractometry for droplet temperature measurements in an ensemble, whereby the rainbow pattern of many individual particles is superimposed onto one image. The nonspherical droplets result in a uniform background and thus do not influence the wanted interference pattern. Performance measures of this system with respect to temperature, size, and nonsphericity are numerous (Vetrano et al. 2006, Saengkaew et al. 2007, Wilms et al. 2008, Saengkaew et al. 2009), but this is no longer a single-particle characterization and falls outside the scope of this review.

2.2.4. Time shift. The time-shift technique, first introduced by Semidetnov (1985) and more widely by Albrecht et al. (1993), is applicable only when the illuminating beam is made to be of the order of the particle size; i.e., the time shift is an effect arising solely from an inhomogeneous illumination of the particle. In principle, a time-of-flight measurement or laser two-focus also exploits a time shift arising from scattering from two separate measurement volumes, albeit detecting the same scattering order. The novelty of the time-shift technique discussed here lies in the fact that the different measurement volumes arise from the same illumination beam but from different scattering orders.

This principle is illustrated schematically in **Figure 8**, shown for a collection angle in backscatter and for a typical liquid droplet (Albrecht et al. 2003). Instead of only one illuminating beam, a laser Doppler system is used, allowing velocity also to be measured. The time shift between various signal parts on one detector is computed as a spatial shift using the velocity information. For a given refractive index, the spatial shift between scattering orders is then a unique function of particle size and detector position. Effectively we are seeing several virtual measurement volumes imaged by the particle onto the detectors. This technique has also been termed the pulse displacement technique (Hess & Wood 1994, Lin et al. 2000), referring to the spatial separation of the signals/measurement volume rather than to the time shift.

The example given in **Figure 8** is appropriate to illustrate some additional possibilities for particle characterization with the time-shift technique. First, the technique works not only in forward scatter but also in near-backscatter, allowing sizing in test sections with only one optical access. The size information is given many times redundantly because not only does the distance between individual signal parts on one detector hold size information, but so does the distance between signal parts on different detectors. Furthermore, the distance between the two signal portions of second-order refraction (i.e., between modes 1 and 2) will be dependent on the refractive index, allowing one to estimate the refractive index. The refractive index may also be a function of temperature; hence a temperature estimate is in principle possible. Finally, the ratio of amplitudes between reflection and refractive orders will be related to the absorption in the particle, which may indicate the concentration of a turbid droplet.

Perhaps even more attractive is the insensitivity of the technique to the nonsphericity of the particle, which is a significant advantage over phase Doppler or rainbow techniques (Damaschke et al. 2002a). Of course, the technique fails if the particle trajectory is such that not all virtual measurement volumes are crossed. The use of laser sheets rather than laser beams can alleviate this difficulty, as indicated in **Figure 8*b*** (Damaschke et al. 2003). The time-shift technique has yet to be demonstrated using fluorescent light.

2.2.5. Pulse delay. Here we discuss a final measurement principle that is generally less well-known and is associated with either very short pulse-width lasers (femtoseconds) or short–coherence length sources. In both cases the pulse width or coherence length is of the order

Figure 8

Principle of the time-shift technique shown for a spherical water droplet detected in backscatter using a laser Doppler system for velocity measurement. (*a*) Five scattering orders are present at this scattering angle: surface wave short path, second-order refraction mode 2, second-order refraction mode 1, reflection, and surface wave long path. (*b*) Each scattering order is seen at a different instant in time as the particle passes through the beams; four are dominant: surface wave short path together with second-order refraction mode 2, second-order refraction mode 1, and reflection. (*c*) The signals resulting from the two detectors. Note that the surface wave long path is just visible in the signal.

of the particle size or smaller. The formulation of a generalized Lorenz-Mie theory for a particle illuminated by laser pulses was first introduced by Gouesbet & Gréhan (2000) and Mees et al. (2001) and subsequently adopted also for Fourier-Lorenz-Mie theory (Damaschke 2003a, Bech & Leder 2004). For Lorenz-Mie scattering, the incoming wave is Fourier decomposed in time and is the sum of a large number of individual continuous-plane waves. The far-field scattered

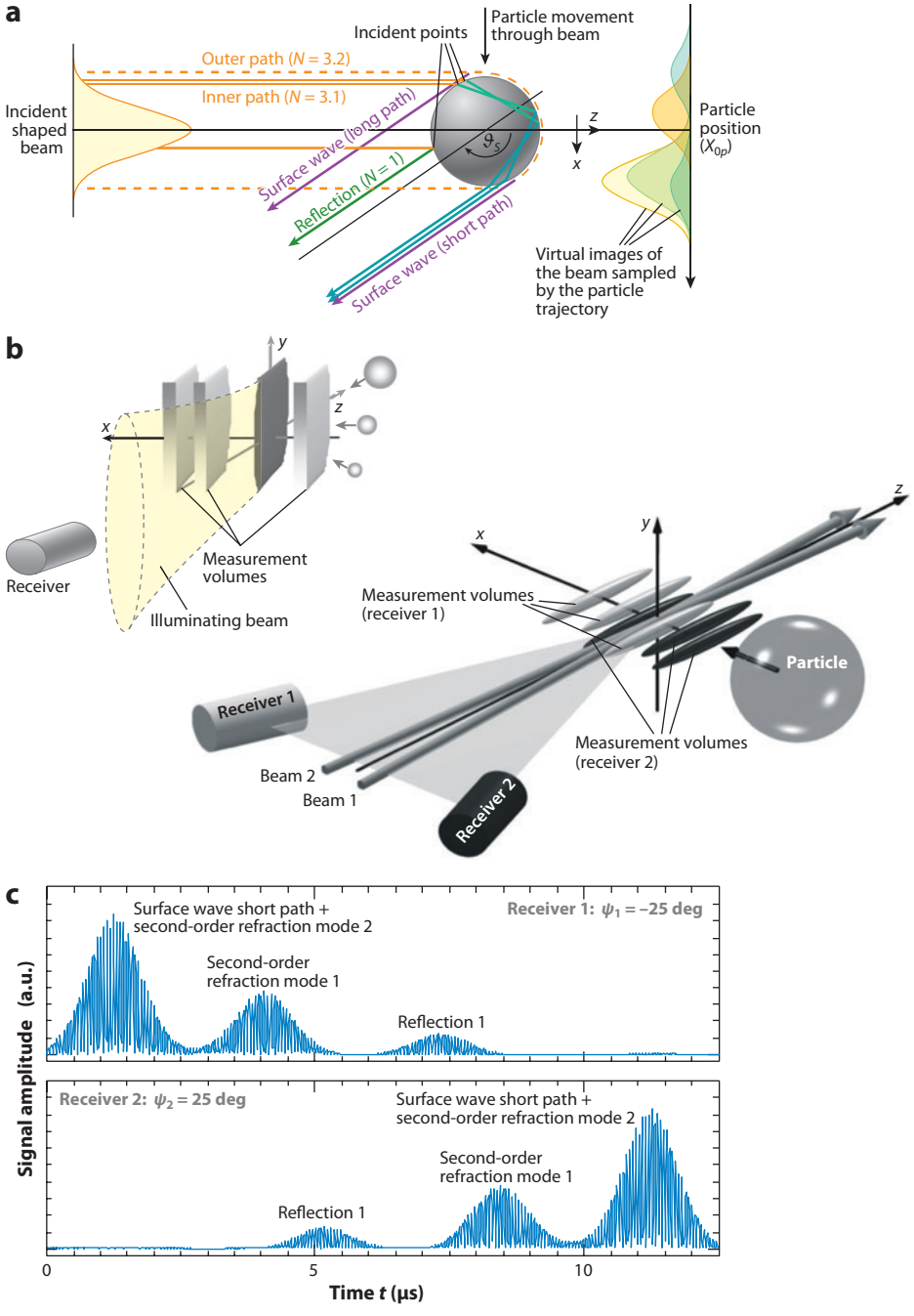

Morphology-dependent resonances: resonances dependent on shape as well as refractive index of material within a particle

field is then the superposition of the scattered field from all these waves. A similar approach is used for shaped beams. The broad bandwidth of a femtosecond laser pulse is equivalent to a short coherence length. Thus, for a pulse length smaller than the difference between the optical path lengths of scattering orders, no far-field interference takes place between the individual scattering orders. The far field is not the superposition of electromagnetic field vectors, but a sum of the intensities of individual scattering orders. This disappearance of scattering lobes is illustrated in **Figure 9** by comparing the far-field angular intensity distribution with continuous-wave illumination to a short pulse illumination (Bakic et al. 2008). Similarly, the nonmonotonic behavior of the scattered intensity with particle size largely disappears. Whether this noninterference is achieved through ultrashort laser pulses, very short–coherence length lasers, or laser diodes is in principle not important, as demonstrated by Peil et al. (2006).

These light-scattering features can be used in diverse manners for particle characterization. The monotonic intensity-size relation is advantageous for intensity-based or intensity-ratio-based techniques, such as Mie/LIF or Mie/planar LIF. Furthermore, morphology-dependent resonances (Johnson 1993), which also hamper intensity-based techniques, disappear because of the short coherence length (Bakic et al. 2008). Perhaps even more intriguing is the use of ultrashort– or short–coherence length pulses in rainbow refractometry, in which case the disturbing ripple structure (**Figure 7**) is suppressed and much higher accuracy can be achieved in the size estimate. This is illustrated in **Figure 10**, which compares the far-field intensity near the first rainbow of a water droplet for continuous-wave illumination with pulse illumination. The feasibility of applying femtosecond laser pulses to rainbow refractometry has been studied in detail by Bakic et al. (2009), who present necessary pulse lengths for given particle-size ranges.

2.2.6. Raman scattering. Raman scattering refers to the modulation of scattered light by the nuclei and electron clouds of the scattering molecules and yields therefore quantitative information about effects of temperature and pressure on these molecules (Schweiger 1990). Because the Raman spectrum is a fingerprint of the molecule, the chemical composition of the sample can also be identified. Although not yet widely applied, spatially resolved Raman scattering has been used to characterize microparticles, exhibiting a number of advantages over other spectroscopic techniques (e.g., LIF and coherent anti-Stokes Raman): (*a*) the simultaneous spatially resolved measurement of the partial densities of all major species, (*b*) simultaneous spatially resolved temperature measurements, (*c*) substantially easier quantification, and (*d*) in some cases (e.g., temperature and fuel/air ratio) the lack of interference from laser power fluctuations and transmission properties of optics because of the use of a ratio of two simultaneously acquired spectral lines (Grünefeld et al. 1994). One major disadvantage is that Raman scattering is a very weak effect; i.e., the scattering cross section, which is the total scattered light flux divided by the incident light flux density, is many orders of magnitude smaller that the scattering cross section for Rayleigh scattering. Thus, high laser power is required to achieve low detection limits, which in turn excite, through morphology-dependent resonances, nonlinear effects (e.g., laser emission, stimulated Raman scattering, four-wave mixing, stimulated Brillouin scattering, and stimulated Rayleigh-wing scattering). Vehring (1998) presented a study to establish the limits of linear Raman scattering.

A majority of studies using Raman spectroscopy have focused on probing single spherical liquid droplets, either levitated or as a droplet chain (Buehler et al. 1991, Fung & Tang 1992, Vehring et al. 1995, Moritz et al. 1997). This is certainly because of the high sensitivity of spontaneous Raman scattering to interfering emissions from other concomitants, for example, in combusting systems. Nevertheless, some studies have demonstrated the use of Raman scattering for multispecies and temperature analysis in spray flames and fired engines (Grünefeld et al. 1994).

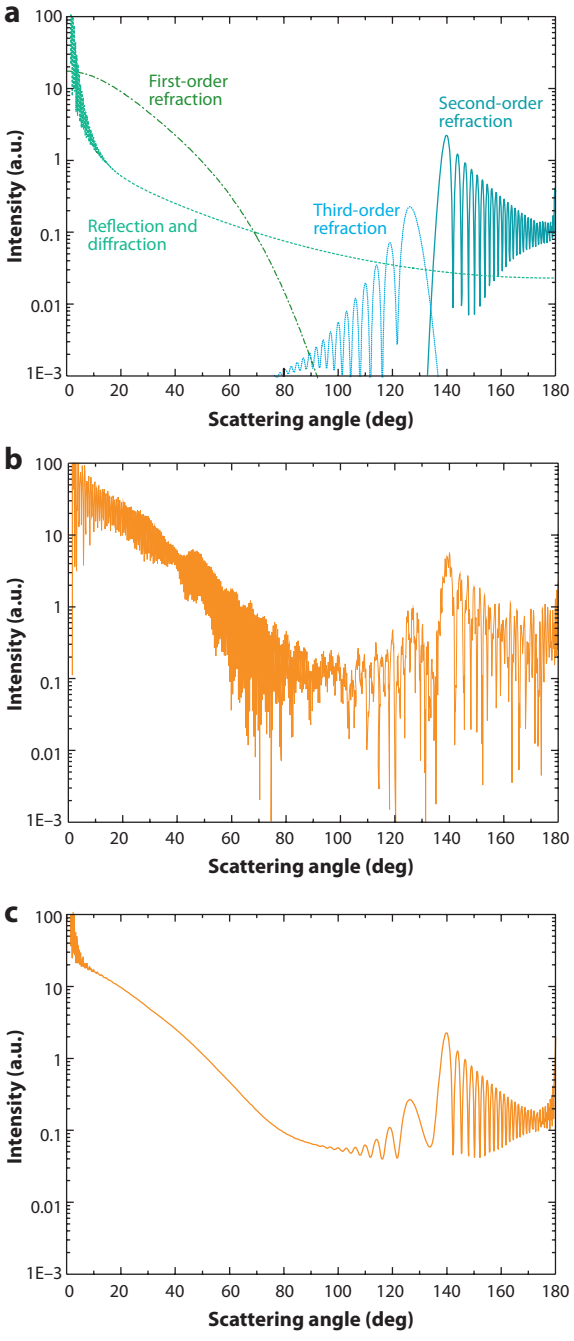

Figure 9

Numerically obtained angular intensity distributions in the far field of a spherical, homogeneous droplet ($d = 94$ μm, $n = 1{,}333$). (*a*) Individual scattering orders, reflection and diffraction (*dashed line*), first-order refraction (*dashed and dotted line*), second-order refraction with the first rainbow (*full line*), and third-order refraction with the second rainbow (*dotted line*). (*b*) The Mie sum is a result of interfering scattering orders for continuous illumination at $\gamma = 780$ nm. (*c*) Simulated 70-fs pulses at a central wavelength of $\gamma = 780$ nm yield a Mie sum, which follows from adding intensities of different scattering orders.

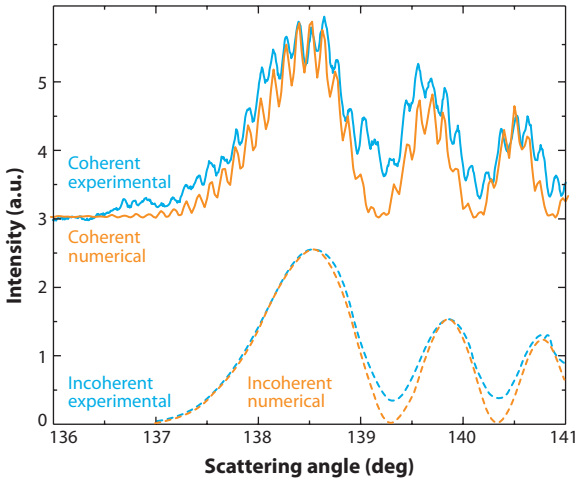

Figure 10

Experimentally (*blue lines*) and numerically (*orange lines*) obtained angular intensity distributions for rainbow refractometry with a water droplet for coherent and incoherent illuminations. The distributions for coherent illumination are shifted upward by three units.

3. SUMMARY AND OUTLOOK

Despite the rather wide variety of techniques reviewed in this article, the overall task of characterizing particles as illustrated in **Figure 1** has only been modestly met. There are several issues representing future challenges.

The need for characterizing sprays is extremely acute, related especially to the energy sector for liquid fuel injection and to the process industry for spray drying. In the former we are dealing not only with liquid fragmentation (i.e., highly nonspherical droplets and ligaments), but also with multicomponent fuels, the components of which exhibit differing rates of evaporation. For reliable prediction of ignition and combustion, the evaporation of fuel sprays and the composition of the fuel mixture must be accurately known, relying on exact measurements for model formulation and validation. Therefore, it is essential to extend diagnostic techniques to capture species concentration in the droplet and vapor concentration in the surrounding gas. This will no doubt require an increased use of techniques depending on inelastic light scattering (i.e., spectroscopic techniques). Similarly, in spray drying, the evaporation rate of complex droplets will provide fundamental information required to properly model the final product's porosity and solubility. This will also require reliable validation data from experiments and, in particular, diagnostics for liquid droplets with high solid content.

In general, the extension of particle characterization to nonspherical shapes is already in high demand. Both direct imaging and digital holography clearly hold great promise in this regard, their development depending to some extent on the sensitivity, resolution, and frame rates of future cameras. Moreover, imaging software to extract particle position and shapes from multiple views is rapidly progressing, and a significant extension to present capabilities can be expected even in the short term.

The remarks in Section 1.3 indicate that substantial progress has been made in a fundamental understanding of light scattering from nonspherical particles; however, this theoretical knowledge is still at a preliminary stage with respect to actual instrument design and development. This is because, in most industrial situations, particles do not possess or keep a unique shape. Even

for a given shape, particles will take on various unknown or random orientations. Therefore, electromagnetic scattering theories for nonspherical particles have mostly been used in offline error analysis for instruments that have assumed a spherical shape but encounter nonspherical particles.

Diagnostics for nonhomogeneous particles are not extensively discussed in this article; indeed these are not abundant. However, there is a strong demand for the development of techniques for layered particles or particles with refractive index steps or gradients. This is not only true for many industrial processes, but also for the extension of optical particle characterization to soft matter, especially cell-like structures. In this field, theories for light scattering also exist. However, measurements in reality remain much more complex.

DISCLOSURE STATEMENT

The author is not aware of any affiliations, memberships, funding, or financial holdings that might be perceived as affecting the objectivity of this review.

ACKNOWLEDGMENTS

The author would like to express his sincere thanks to numerous colleagues and former graduate students with whom he has interacted in this field, specifically, Prof. H.-E. Albrecht, Prof. N. Damaschke, Prof. F. Durst, Dr. B. Frackowiak, Prof. G. Gouesbet, Dr. G. Gréhan, Dr. I.V. Roisman, Dr. N. Semidetnov, and Dr. F. Xu. Furthermore, the author would like to gratefully acknowledge the financial support of the Deutsche Forschungsgemeinschaft through numerous research grants.

LITERATURE CITED

Adrian RJ, Westerweel J. 2010. *Particle Image Velocimetry*. Cambridge, UK: Cambridge Univ. Press

Aísa L, Garcia JA, Cerecedo LM, García Palacín I, Clavo E. 2002. Particle concentration and local mass flux measurements in two-phase flows with PDFA: application to the study on the dispersion of spherical particles in a turbulent air jet. *Int. J. Multiphase Flow* 28:301–24

Aizu Y, Durst F, Gréhan G, Onofri F, Xu T-H. 1993. PDA system without Gaussian beam defects. In *Proc. 3rd Int. Congr. Opt. Part. Sizing, Yokohama, Japan*, ed. M Maeda, pp. 461–70. Hiyoshi, Japan: Keio Univ., Dep. Mech. Eng.

Albrecht H-E, Bech H, Damaschke N, Felcke M. 1995. Die Berechnung der Streuintensität eines beliebig im Laserstrahl positionierten Teilchens mit Hilfe der zweidimensionalen Fouriertransformation. *Optik* 100:118–24

Albrecht H-E, Borys M, Damaschke N, Tropea C. 2003. *Laser Doppler and Phase Doppler Measurement Techniques*. Heidelberg: Springer-Verlag

Albrecht H-E, Borys M, Hübner K. 1993. Generalized theory for the simultaneous measurement of particle size and velocity using laser Doppler and laser two-focus methods. *Part. Part. Syst. Charact.* 10:138–45

Albrecht H-E, Borys M, Wenzel M. 1996. Influence of the measurement volume on the phase error in phase Doppler anemometry, part 2: analysis by extension of geometrical optics to the laser beam; refractive mode operation. *Part. Part. Syst. Charact.* 13:18–26

Anders K, Roth N, Frohn A. 1991. Simultaneous in situ measurements of size and velocity of burning droplets. *Part. Part. Syst. Charact.* 8:136–41

Asano S, Yamamoto G. 1975. Light scattering by a spheriodal particle. *Appl. Opt.* 14:29–49

Bachalo WD. 1980. A method for measuring the size and velocity of spheres by dual beam light scatter interferometry. *Appl. Opt.* 19:363–70

Bachalo WD, Houser MJ. 1984. Phase/Doppler spray analyser for simultaneous measurement of drop size and velocity distributions. *Opt. Eng.* 23:583–90

Bakic S, Heinisch C, Damaschke N, Tschudi T, Tropea C. 2008. Time integrated detection of femtosecond laser pulses scattered by small droplets. *Appl. Opt.* 467:523–30

Bakic S, Xu F, Damsachke N, Tropea C. 2009. Feasibility of extending rainbow refractometry to small particles using femtosecond laser pulses. *Part. Part. Syst. Charact.* 26:34–40

Barton J. 1997. Electromagnetic-field calculations for a sphere illuminated by a higher-order Gaussian beam. I. Internal and near-field effects. *Appl. Opt.* 36:1303–11

Bauckhage K, Flögel H. 1984. Simultaneous measurement of droplet size and velocity in nozzle sprays. In *Proc. 2nd Int. Symp. Laser Anemometry Fluid Mech., Lisbon, Portugal*, ed. DFG Durão, RJ Adrian, F Durst, H Mishina, JH Whitelaw, Pap. 18.1. Lisbon: LADOAN

Bazile R, Stepowski D. 1994. Measurements of the vaporization dynamics in the development zone of a burning spray by planar laser induced fluorescence and Raman scattering. *Exp. Fluids* 16:171–80

Bazile R, Stepowski D. 1995. Measurements of vaporized and liquid fuel concentration fields in a burning spray jet of acetone using planar laser induced fluorescence. *Exp. Fluids* 20:1–9

Bech H, Leder A. 2004. Particle sizing by ultrashort laser pulses: numerical simulation. *Optik* 115:205–17

Black DL, McQuay MQ, Bonin M. 1996. Laser-based techniques for particle-size measurement: a review of sizing methods and their industrial applications. *Prog. Energy Combust. Sci.* 22:267–306

Bongiovanni C, Chevallier JPh, Fabre J. 1997. Sizing of bubbles by incoherent imaging: defocus bias. *Exp. Fluids* 23:209–16

Borys M, Schelinsky B, Albrecht H-E, Krambeer H. 1998. Light scattering analysis with methods of geometrical optics for a particle arbitrarily positioned in a laser beam. *Optik* 198:137–50

Buehler MF, Allen TM, Davis EF. 1991. Microparticle Raman spectroscopy of multicomponent aerosols. *J. Colloid Interface Sci.* 146:79–89

Castanet G, Delconte A, Lemoine F, Mees L, Gréhan G. 2005. Evaluation of temperature gradients within combusting droplets in linear stream using two colors laser-induced fluorescence. *Exp. Fluids* 39:431–40

Castanet G, Lavieille P, Lebouché M, Lemoine F. 2003. Measurement of the temperature distribution within monodisperse combusting droplets in linear streams using two-color laser-induced fluorescence. *Exp. Fluids* 35:563–71

Choo YJ, Kang BS. 2006. The characteristics of the particle position along an optical axis in particle holography. *Meas. Sci. Technol.* 17:761–70

Coppeta J, Rogers C. 1998. Dual emission laser induced fluorescence for direct planar scalar behavior measurements. *Exp. Fluids* 25:1–15

Damaschke N. 2003a. *Light scattering theories and their use for single particle characterization*. PhD diss. Tech. Univ. Darmstadt, Ström. Aerodyn.

Damaschke N. 2003b. Particle sizing. In *Handbook of Laser Technology and Applications*, ed. CE Webb, JDC Jones, pp. 1931–50. Bristol: Inst. Phys. Publ.

Damaschke N, Gouesbet G, Gréhan B, Mignon H, Tropea C. 1998. Response of phase Doppler anemometer systems to nonspherical droplets. *Appl. Opt.* 37:1752–61

Damaschke N, Nobach H, Nonn TI, Semidetnov N, Tropea C. 2005. Multi-dimensional particle sizing techniques. *Exp. Fluids* 39:336–50

Damaschke N, Nobach H, Semidetnov N, Tropea C. 2002a. Optical particle sizing in backscatter. *Appl. Opt.* 41:5713–27

Damaschke N, Nobach H, Semidetnov N, Tropea C. 2003. Laser Doppler based particle characterization with backscattered light. In *9th Int. Congr. Liquid Atomiz. Spray Systems, Sorrento, Italy*, ed. A Cavaliere, Pap. 10-1. Naples, Italy: ILASS-Europe

Damaschke N, Nobach H, Tropea C. 2002b. Optical limits of particle concentration for multi-dimensional particle sizing techniques in fluid mechanics. *Exp. Fluids* 32:143–52

Debye (Debije) P. 1908. Das elektromagnetische Feld um einen Zylinder und die Theorie des Regenbogens. *Phys. Z.* 9:775–78

Denis L, Fourner T, Ducottet C. 2005. Twin-image noise reduction by phase retrieval in in-line digital holography. *Proc. SPIE* 5814:141–61

Deprédurand V, Miron P, Labergue A, Wolff M, Castanet G. 2008. A temperature-sensitive tracer suitable for two-color laser-induced fluorescence thermometry applied to evaporating fuel droplets. *Meas. Sci. Technol.* 19:105403

Doicu A, Wriedt T, Ermin YA. 2000. *Acoustic and Electromagnetic Scattering Analysis Using Discrete Sources*. New York: Academic

Domann R, Hardalupas Y. 2001a. Spatial distribution of fluorescence intensity within large droplets and its dependence on dye concentration. *Appl Opt.* 40:3586–97

Domann R, Hardalupas Y. 2001b. A study of parameters that influence the accuracy of the planar droplet sizing technique. *Part. Part. Syst. Charact.* 18:3–11

Domann R, Hardalupas Y. 2003. Quantitative measurement of planar droplet Sauter mean diameter in sprays using planar droplet sizing. *Part. Part. Syst. Charact.* 20:209–18

Dubois F, Schockaert C, Callens N, Yourassowsky C. 2006. Focus plane detection criteria in digital holography microscopy by amplitude analysis. *Opt. Exp.* 14:5895–980

Dullenkopf K, Willmann M, Wittig S, Schöne F, Stieglmeier M, et al. 1998. Comparative mass flux measurement in sprays using patternator and the phase Doppler technique. *Part. Part. Syst. Charact.* 15:81–89

Durst F, Naqwi A. 1990. Optical methods for studies of multiphase flows. In *Proc. 2nd Int. Congr. Opt. Part. Sizing, Tempe, Arizona*, ed. ED Hirleman, pp. 269–76. Tempe: Arizona State Univ. Press

Düwel I, Schorr J, Wolfrum J, Schulz C. 2003. Laser-induced fluorescence of tracers dissolved in evaporating droplets. *Appl. Phys. B* 78:127–31

Farmer WM. 1972. Measurement of particle size, number density, and velocity using a laser interferometer. *Appl. Opt.* 11:2603–12

Flögel HH. 1981. *Untersuchung von Teilchengeschwindigkeit und Teilchengröße mit einem Laser-Doppler-Anemometer*. PhD diss. Univ. Bermen, Germany

Frackowiak B, Tropea C. 2010a. Fluorescence modelling of droplets intersecting a focussed laser beam. *Opt. Lett.* 35:1386–88

Frackowiak B, Tropea C. 2010b. Numerical analysis of the diameter influence on droplet fluorescence. *Appl. Opt.* 49:2363–70

Fung KH, Tang IN. 1992. Aerosol particle analysis by resonance Raman spectroscopy. *J. Aerosol Sci.* 23:301–7

Garcia-Sucerquia J, Xu W, Jericho SK, Klages P, Jericho MH, Kreuzer HJ. 2006. Digital in-line holographic microscopy. *Appl. Opt.* 43:836–50

Glantsching WJ, Chen SH. 1981. Light scattering from water droplets in the geometrical optics approximation. *Appl. Opt.* 20:2499–509

Glover AR, Skippon SM, Boyle RD. 1995. Interferometric laser imaging for droplet sizing: a method for droplet-size measurement in sparse spray systems. *Appl. Opt.* 34:8409–21

Gouesbet G. 2009. Generalized Lorenz-Mie theories, the third decade: a perspective. *J. Quant. Spectrosc. Radiat. Transf.* 110:1223–38

Gouesbet G, Gréhan G. 1982. Sur la généralisation de la théorie de Lorenz-Mie. *J. Opt.* 13(2):97–103

Gouesbet G, Gréhan G. 2000. Generic formulation of a generalized Lorenz-Mie theory for a particle illuminated by laser pulses. *Part. Part. Syst. Charact.* 17:213–24

Gouesbet G, Gréhan G. 2010. *Scattering of Arbitrary Shaped Beams by Regular Particles* (*Generalized Lorenz-Mie Theories*). Heidelberg: Springer-Verlag

Gouesbet G, Maheu B, Gréhan G. 1988. Light scattering from a sphere arbitrarily located in a Gaussian beam, using a Bromwich formulation. *J. Opt. Sci. Am. A* 5(9):1427–43

Gréhan G, Gouesbet G, Naqwi A, Durst F. 1993. Particle trajectory effects in phase Doppler systems: computations and experiments. *Part. Part. Syst. Charact.* 10:332–38

Grünefeld G, Beushausen V, Andresen P, Hentschel W. 1994. Spatially resolved Raman scattering for multi-species and temperature analysis in technically applied combustion systems: spray flame and four-cylinder in-line engine. *Appl Phys. B* 58:333–42

Hain R, Kähler C, Tropea C. 2007. Comparison of CCD, CMOS and intensified cameras. *Exp. Fluids* 42:403–11

Hardalupas Y, Hishida K, Maeida M, Morikita H, Taylöor AMKP, Whitelaw JH. 1994. Shadow Doppler technique for sizing particles of arbitrary shape. *Appl. Opt.* 33:8417–26

Hardalupas Y, Sahu S, Taylor AMKP, Zarogoulidis K. 2010. Simultaneous planar measurement of droplet velocity and size with gas phase velocities in a spray by combined ILIDS and PIV techniques. *Exp. Fluids* 49:417–34

Harrington RF. 1968. *Field Computation by Moment Methods*. New York: Macmillan

Hecht E, Zajac A. 2003. *Optics*. Amsterdam: Addison-Wesley Longman

Hess CF. 1998. Planar particle image analyzer. In *Proc. 9th Int. Symp. Appl. Laser Technol. Fluid Mech., Lisbon, Portugal*, ed. RJ Adrian, DFG Durão, F Durst, MV Heitor, M Maeda, JH Whitelaw, Pap. 18.1. Lisbon: Inst. Super. Tec.

Hess CF, L'Esperance D. 2009. Droplet imaging velocimeter and sizer: a two-dimensional technique to measure droplet size. *Exp. Fluids* 47:171–82

Hess CF, Wood CP. 1994. The pulse displacement technique: a single particle counter with a size range larger than 1000:1. *Part. Part. Syst. Charact.* 11:107–13

Heydt M, Rosenhahn A, Grunze M, Pettitt M, Callow ME, Callow JA. 2007. Digital in-line holography as a three-dimensional tool to study motile marine organisms during their exploration of surfaces. *J. Adhes.* 83:417–30

Hishida K, Sakakibara J. 2000. Combined planar laser-induced fluorescence-particle image velocimetry technique for velocity and temperature fields. *Exp. Fluids* 29:S129–40

Hofeldt DL. 1993. Full-field measurements of particle size distributions: I. theoretical limitations of the polarization ratio method. *Appl. Opt.* 32:7551–58

Hofeldt DL, Hanson RK. 1991. Instantaneous imaging of particle size and spatial distribution in two-phase flows. *Appl. Opt.* 30:4936–48

Hovenac EA, Lock JA. 1992. Assessing the contributions of surface waves and complex rays to far-field Mie scattering by use of the Debye series. *J Opt. Soc. Am. A* 9:781–95

Jermy MC, Greenhalgh DA. 2000. Planar dropsizing by elastic and fluorescence scattering in sprays too dense for phase Doppler measurement. *Appl. Phys. B* 71:703–10

Johnson BR. 1993. Theory of morphology-dependent resonances: shape resonances and width formulas. *J. Opt. Soc. Am. A* 10:343–52

Jones AR. 1999. Light scattering for particle characterization. *Prog. Energy Combust. Sci.* 25:1–53

Jones AR, Parasram NT, Taylor AMKP. 2002. Numerical simulation of the sizing performance of the shadow Doppler velocimeter (SDV). *Meas. Sci. Technol.* 13:317–30

Jones AR, Sarjeant M, Davis CR, Deham RO. 1978. Application of in-line holography to drop size measurement in dense fuel sprays. *Appl. Opt.* 17:328–30

Kawaguchi T, Akasaka Y, Maeda M. 2002. Size measurement of droplets and bubbles by advanced interferometric laser imaging technique. *Meas. Sci. Technol.* 13:308–16

Kerker M, ed. 1988. *Selected Papers on Light Scattering. Parts 1 and 2*. Bellingham, WA: SPIE

Kim S, Lee SJ. 2006. Effect of particle concentration on digital holographic PTV measurement. *J. Korean Soc. Mech. Eng. B* 30:929–34

Kogelnik H, Li T. 1966. Laser beams and resonators. *Appl. Opt.* 5:1550–67

König G, Anders K, Frohn A. 1986. A new light-scattering technique to measure the diameter of periodically generated moving droplets. *J. Aerosol Sci.* 17:157–67

Kühn J, Charrière F, Colomb T, Cuche E, Montfort F, et al. 2008. Axial subnanometer accuracy in digital holographic microscopy. *Meas. Sci. Technol.* 19:074007

Labergue A, Delconte A, Lemoine F. 2008. Three-color laser induced fluorescence applied to temperature measurements in sprays. In *14th Symp. Appl. Laser Technol. Fluid Mech., Lisbon, Portugal*, ed. RJ Adrian, DFG Durão, K Hishida, AL Moreira, C Tropea, Pap. 10.2.4. Lisbon: Inst. Super. Tec.

Labergue A, Deprédurand V, Delconte A, Castanet G, Lemoine F. 2010. New insight into two-color LIF thermometry applied to temperature measurements of droplets. *Exp. Fluids* 49:547–56

Lavieille P, Delconte A, Blondel D, Lebouché M, Lemoine F. 2004. Non-intrusive temperature measurements using three-color laser-induced fluorescence. *Exp. Fluids* 36:706–16

Lavieille P, Lemoine F, Lavergne G, Lebouché M. 2001. Evaporating and combusting droplet temperature measurements using two-color laser-induced fluorescence. *Exp. Fluids* 31:45–55

Lefebvre CB, Coëtmellec S, Lebrun D, Özkul C. 2000. Application of wavelet transform to hologram analysis: three-dimensional location of particles. *Opt. Laser Eng.* 33:409–21

Lemoine F, Antoine Y, Wolff M, Lebouché M. 1999. Simultaneous temperature and 2D velocity measurements in a turbulent heated jet using combined laser-induced fluorescence and LDA. *Exp. Fluids* 26:315–23

Lin SM, Waterman DR, Lettington AH. 2000. Measurement of droplet velocity, size and refractive index using the pulse displacement technique. *Meas. Sci. Technol.* 11:L1–4

Lorenz L. 1890. Lysbevaegeisen i og uden for en hal plane lysbôlger belyst kluge. *Vidensk. Selk Skr.* 6:1–62

Ludwig AC. 1991. The generalized multipole technique. *Comput. Phys. Commun.* 68:306–14

Maeda M, Akasaka Y, Kawaguchi T. 2002. Improvements of the interferometric technique for simultaneous measurement of droplet size and velocity vector field and its application to a transient spray. *Exp. Fluids* 33:125–34

Maeda M, Kawaguchi T, Hishida K. 2000. Novel interferometric measurement of size and velocity distributions of spherical particles in fluid flows. *Meas. Sci. Technol.* 11:L13–18

Maqua C, Depredurand V, Castanet G, Wolff M, Lemoine F. 2007. Composition measurement of bicomponent droplets using laser-induced fluorescence of acetone. *Exp. Fluids* 43:979–92

Marsten PL. 1980. Rainbow phenomena and the detection of nonsphericity in drops. *Appl. Opt.* 19:680–85

Matsuura K, Komaki M, Ueyama K, Hironaga K. 2004. Shadow Doppler velocimetry with double fiber-array sensors. *Exp. Fluids* 36:11–22

Mees L, Gréhan G, Gouesbet G. 2001. Time-resolved scattering diagrams for a sphere illuminated by plane wave and focused short pulses. *Opt. Commun.* 194:59–65

Men A, Krimerman Y, Adler D. 1981. A new method of simultaneous particle sizing and two-component velocity measurement. *J. Phys. E* 14:747–51

Mie G. 1908. Beiträge zur Optik trüber Medien, speziell kolloidaler Metallösungen. *Ann. Phys.* 25(4):277–452

Mishchenko MI, Hovenier JW, Travis LD, eds. 2000. *Light Scattering by Nonspherical Particles: Theory, Measurements, and Applications*. San Diego: Academic

Morikita H, Taylor AMKP. 1998. Application of shadow Doppler velocimetry to paint spray: potential and limitations in sizing optically inhomogeneous droplets. *Meas. Sci. Technol.* 9:221–31

Moritz H, Lange S, Schweiger G. 1997. The radial weighting of concentration profiles inside of microparticles by Raman spectroscopy. *J. Aerosol Sci.* 28:199–200

Müller J, Kebbel V, Jüptner W. 2004. Characterization of spatial particle distributions in a spray-forming process using digital holography. *Meas. Sci. Technol.* 15:707–10

Murray MA, Melton LA. 1985. Fluorescence methods for determination of temperature in fuel spray. *App. Opt.* 24:2783–87

Naqwi A, Durst F, Liu X. 1991. Two optical methods for simultaneous measurement of particle size, velocity, and refractive index. *Appl. Opt.* 30:4949–59

Nussenzveig HM. 1969a. High-frequency scattering by a transparent sphere. I. Direct reflection and transmission. *J. Math. Phys.* 10:82–124

Nussenzveig HM. 1969b. High-frequency scattering by a transparent sphere. II. Theory of the rainbow and the glory. *J. Math. Phys.* 10:125–76

Onofri F, Bergounoux L, Firpo JL, Misguish-Ripault J. 1998. Velocity, size and concentration in suspension measurements of cylindrical jets and spherical droplets. In *Proc. 9th Int. Symp. Appl. Laser Technol. Fluid Mech. Lisbon, Portugal*, ed. RJ Adrian, DFG Durão, F Durst, MV Heitor, M Maeda, JH Whitelaw, Pap. 9.2. Lisbon: Inst. Super. Tec.

Onofri F, Girasole T, Gréhan G, Gouesbet G, Brenn G, et al. 1996. Phase-Doppler anemometry with dual burst technique for measurements of refractive index and absorption coefficient simultaneously with size and velocity. *Part. Part. Syst. Charact.* 13:112–24

Palero V, Arroyo MP, Soria J. 2007. Digital holography for microdroplet diagnostics. *Exp. Fluids* 43:185–95

Palero V, Lobera J, Arroyo MP. 2005. Digital image plane holography (DIPH) for two-phase flow diagnostics in multiple planes. *Exp. Fluids* 39:397–406

Peil M, Fischer I, Elsäßer W, Bakic S, Damschke N, et al. 2006. Rainbow refractometry with a tailored incoherent semiconductor laser source. *Appl. Phys. Lett.* 89:091106

Pitcher G, Wigley G, Saffman M. 1990. Sensitivity of drop size measurements by phase Doppler anemometry to refractive index changes in combusting fuel sprays. In *Proc. 5th Int. Symp. Appl. Laser Technol. Fluid Mech.*, *Lisbon*, *Portugal*, ed. DFG Durão, RJ Adrian, M Maeda, F Durst, JH Whitelaw, Pap. 14.4. Lisbon: Inst. Super. Tec.

Purcell EM, Pennypacker CR. 1993. Scattering and absorption of light by nonspherical dielectric grains. *Astrophys. J.* 186:705–14

Qiu HH, Hsu CT. 1999. Method of phase-Doppler anemometry free from the measurement volume effect. *Appl. Opt.* 38:2737–42

Raffel M, Willert C, Wereley S, Kompenhans J. 2007. *Particle Image Velocimetry: A Practical Guide*. Hedielberg: Springer-Verlag

Ragucci R, Cavaliere A, Massoli P. 1990. Drop sizing by laser light scattering exploiting intensity angular oscillation in the Mie regime. *Part. Part. Syst. Charact.* 7:221–25

Roisman IV, Tropea C. 2001. Flux measurements in sprays using phase Doppler techniques. *Atom. Sprays* 11:673–705

Roth N, Anders K, Frohn A. 1991. Refractive-index measurements for the correction of particle sizing methods. *Appl. Opt.* 30:4960–65

Roth N, Anders K, Frohn A. 1996. Size insensitive rainbow refractometry: theoretical aspects. In *Proc. 8th Int. Symp. Appl. Laser Technol. Fluid Mech.*, *Lisbon*, *Portugal*, ed. RJ Adrian, DFG Durão, F Durst, MV Heitor, M Maeda, JH Whitelaw, Pap. 9.2. Lisbon: Inst. Super. Tec. x

Saengkaew S, Charinpanikul T, Laurent C, Biscos Y, Lavergne G, et al. 2010. Processing of individual rainbow signals. *Exp. Fluids* 48:111–19

Saengkaew S, Charinpanitkul T, Vanisri H, Tanthapanichakoon W, Biscos Y, et al. 2007. Rainbow refractrometry on particles with radial refractive index gradients. *Exp. Fluids* 43:595–601

Saengkaew S, Godard G, Blaisot JB, Gréhan G. 2009. Experimental analysis of global rainbow technique: sensitivity of temperature and size distribution measurements to nonspherical droplets. *Exp. Fluids* 47:839–48

Saffman M. 1986. The use of polarized light for optical particle sizing. In *Proc. 3rd Int. Symp. Appl. Laser Anemometry Fluid Mech.*, *Lisbon*, *Portugal*, ed. DFG Durão, RJ Adrian, F Durst, T Asanuma, JH Whitelaw, Pap. 18-2. Lisbon: LADOAN

Saffmann M, Buchhave P, Tanger H. 1984. Simultaneous measurement of size, concentration and velocity of spherical particles by a laser Doppler method. In *Proc. 2nd Int. Symp. Laser Anemometry Fluid Mech.*, *Lisbon*, *Portugal*, ed. DFG Durão, RJ Adrian, F Durst, H Mishina, JH Whitelaw, Pap. 8.1. Lisbon: LADOAN

Sankar SV, Bachalo WD. 1991. Response characteristics of the phase Doppler particle analyzer for sizing spherical particles larger than the light wavelength. *Appl. Opt.* 30:1487–96

Sankar SV, Ibrahim KM, Buermann DH, Fidrich JM, Bachalo WD. 1993. An integrated phase Doppler/rainbow refractometer system for simultaneous measurement of droplet size, velocity and refractive index. In *3rd Int. Conf. Opt. Part. Sizing*, *Yokohama*, *Japan*, ed. M Maeda, pp. 275–83. Hiyoshi, Japan: Keio Univ., Dep. Mech. Eng.

Sankar SV, Inenaga A, Bachalo WD. 1992. Trajectory dependent scattering in phase Doppler interferometry: minimizing and eliminating sizing error. In *Proc. 6th Int. Symp. Appl. Laser Technol. Fluid Mech.*, *Lisbon*, *Portugal*, ed. RJ Adrian, DFG Durão, F Durst, MV Heitor, M Maeda, JH Whitelaw, Pap. 1.2. Lisbon: Inst. Super. Tec.

Schnars U, Jüptner WPO. 2002. Digital recording and numerical reconstruction of holograms. *Meas. Sci. Technol.* 13:R85–101

Schnars U, Jüptner W. 2005. *Digital Holography*. Berlin: Springer-Verlag

Schodl R, Förster W. 1988. A multi-color fiber optic laser two focus velocimeter for 3 dimensional flow analysis. In *Proc. 4th Int. Symp. Appl. Laser Anemometry Fluid Mech.*, *Lisbon*, *Portugal*, ed. DFG Durão, RJ Adrian, T Asanuma, F Durst, JH Whitelaw, Pap. 4.2. Lisbon: Inst. Super. Tec.

Schulz C, Sick V. 2005. Tracer-LIF diagnostics: quantitative measurement of fuel concentration, temperature and air/fuel ratio in practical combustion situations. *Prog. Energy Combust. Sci.* 31:75–121

Schweiger G. 1990. Raman scattering on single aerosol particles and on flowing aerosols: a review. *J. Aerosol Sci.* 21:483–509

Semidetnov N. 1985. *Investigation of laser Doppler anemometer as instrumentation for two-phase flow measurements*. PhD diss. Leningrad Inst. Precis. Mech. Optics, Dep. Opto-Electron. Instrum.
Semidetnov N, Tropea C. 2004. Conversion relationships for multidimensional particle sizing techniques. *Meas. Sci. Technol.* 15:112–18
Sheng J, Katz J. 2010. Applications of holography in fluid mechanics and particle dynamics. *Annu. Rev. Fluid Mech.* 42:531–55
Sheng J, Malkeil E, Katz J. 2006. Digital holographic microscope for measuring three-dimensional particle distributions and motions. *Appl. Opt.* 45:3893–901
Sheng J, Malkiel E, Katz J, Adolf J, Belas R, Place AR. 2007. Digital holographic microscopy reveals prey-induced changes in swimming behavior of predatory dinoflagellates. *Proc. Natl. Acad. Sci. USA* 104:17512–17
Shimizu I, Shimoda M, Suzuki T, Emori Y. 1982. A light scattering and holographic technique for determining droplet size and volume density distribution in diesel fuel sprays. *Soc. Automot. Eng. Pap. 820355*, Warrendale, PA
Singh VR, Asundi AK. 2005. Amplitude contrast image enhancement in digital holography for particles analysis. *Proc. SPIE* 5878:587817
Thompson BJ. 1974. Holographic particle sizing techniques. *J. Phys. E* 7:781–88
Tropea C, Xu T-H, Onofri F, Gréhan G, Haugen P, Stieglmeier M. 1996. Dual-mode phase-Doppler anemometer. *Part. Part. Syst. Charact.* 13:165–70
van Beeck JPAJ, Giannoulis D, Zimmer L, Riethmuller M. 1999. Global rainbow refractometry for droplet temperature measurement. *Opt. Lett.* 24:2696–98
van Beeck JPAJ, Riethmuller ML. 1996. Rainbow phenomena applied to the measurement of droplet size and velocity and to the detection of nonsphericity. *Appl. Opt.* 35:2259–66
van Beeck JPAJ, Zimmer ML, Riethmuller ML. 2001. Global rainbow thermometry for mean temperature and size measurement of spray droplets. *Part. Part. Syst. Charact.* 18:196–204
van de Hulst HC. 1981. *Light Scattering by Small Particles*. New York: Dover
van de Hulst HC, Wang RT. 1991. Glare points. *Appl. Opt.* 30:4755–63
Van Der Pol B, Bremmer H. 1937. Diffraction of electromagnetic waves from a point source. *Philos. Mag.* 24:141–90; 825–64
Vehring R. 1998. Linear Raman spectroscopy on aqueous aerosols: influence of nonlinear effect on detection limits. *J. Aerosol Sci.* 29:65–79
Vehring R, Moritz H, Niekamp D, Heinrich P, Schweiger G. 1995. Linear Raman spectroscopy in droplet chains: a new experimental method for the analysis of fast transport processes and reactions on microparticles. *Appl. Spectrosc.* 49:1215–24
Vetrano MR, Gauthier S, van Beeck J, Boulet P, Buchlin M-M. 2006. Characterization of a nonisothermal water spray by global rainbow thermometry. *Exp. Fluids* 40:15–22
Volakis JL, Chatterjee A, Kempel LC. 1994. Review of the finite-element method for three-dimensional electromagnetic scattering. *J. Opt. Soc. Am. A* 11:1422–33
Volkholz P, Melling A, Durst F. 1998. Refractive index measurements with phase Doppler anemometry in the size range 0.3 to 20 μm. In *Proc. 9th Int. Symp. Appl. Laser Technol. Fluid Mech., Lisbon, Portugal*, ed. RJ Adrian, DFG Durão, F Durst, MV Heitor, M Maeda, JH Whitelaw, Pap. 9.1. Lisbon: Inst. Super. Tec.
Widmann JF, Presser C, Leigh SD. 2001. Improving phase Doppler volume flux measurements in low data rate applications. *Meas. Sci. Technol.* 12:1180–90
Wilms J, Gréhan G, Lavergne G. 2008. Global rainbow refractometry with a selective imaging method. *Part. Part. Syst. Charact.* 25:39–48
Wriedt T. 1998. A review of elastic light scattering theories. *Part. Part. Syst. Charact.* 15:67–74
Xu F, Lock JA, Gouesbet G. 2010. Debye series for light scattering by a nonspherical particle. *Phys. Rev. A.* 81:043824
Xu F, Ren KF, Cai X. 2006. Extended geometrical-optics approximation to on-axis Gaussian beam scattering. I. By a spherical particle. *Appl. Opt.* 45:4990–99
Xu T-H, Tropea C. 1994. Improving the performance of two-component phase Doppler anemometers. *Meas. Sci. Technol.* 5:969–75

Yee KS. 1966. Numerical solution of initial boundary value problem involving Maxwell's equations in isotropic media. *IEEE Trans. Antenn. Prop.* 14:302–7

Yeh C-N, Kosaka H, Kamimoto T. 1993. A fluorescence/scattering imaging technique for instantaneous 2D measurements of particle size distribution in a transient spray. In *Proc. 3rd Congr. Opt. Part. Sizing, Yokohama, Japan*, ed. M Maeda, pp. 355–61. Hiyoshi, Japan: Keio Univ., Dep. Mech. Eng.

Annual Review of
Fluid Mechanics

Volume 43, 2011

Contents

Indexes

Errata

An online log of corrections to *Annual Review of Fluid Mechanics* articles may be found at http://fluid.annualreviews.org/errata.shtml